Journal of ELECTRICAL ENGINEERING, VOL 70 (2019), NO-7S, 77–82

sciendo

PAPERS

On KCN treatment effects on optical properties of Si-based bilayers

Jarmila Müllerová[*], Emil Pinčík[**], Martin Králik[*], Michaela Holá[*], Masao Takahashi[*,⊞], Hikaru Kobayashi[***]**

In this paper we report results from optical transmittance spectroscopy complemented with data from Raman scattering measurements to determine optical properties of two series of silicon based bilayers deposited by PECVD on glass substrate (intrinsic a-Si:H/p-type a-SiC:H and n-type mc-Si:H/intrinsic a-Si:H). These samples represent segments of common p-i-n thin film amorphous silicon solar cells with intrinsic hydrogenated silicon (a-Si:H) as the solar absorber. The members of the series differ by the KCN treatment conditions. Dispersive and absorptive optical properties – refractive indices, absorption coefficients and optical band gaps were determined from transmittance spectra. Each bilayer was considered as one effective thin film the optical properties of which can be regarded as effective optical properties of the bilayer structure. After KCN treatments refractive indices were modified probably due to the structural changes of bilayers. Moreover the effect of the solvent used in KCN solutions was recognized. Optical band gaps calculated either by the Tauc procedure or determined as iso-absorption levels were found to be only slightly KCN treatment dependent.

K e y w o r d s: KCN treatment, effective thin film, bilayers, silicon, refractive index, optical band gap

1 Introduction

Thin film structures based on amorphous (a-Si) or microcrystalline (mc-Si) thin film silicon have become reliable materials in many electronic and optoelectronic devices, such as solar cells, thin film transistors (TFF), LCD *etc* [1-3]. In a-Si and mc-Si solar cells conversion efficiency and its stability are strategic issues because their optical and electrical properties suffer from light-induced degradation caused by dangling or week bonds [4].

Therefore several techniques have been developed to passivate defects, mainly based on beneficial effects of hydrogen. Among wet passivation techniques cyanide method including immersion of semiconductor structures in dilute cyanide solutions was successfully applied enabling also metal species removal in addition [5-8]. The principle is that surface defect states are passivated by Si-CN bonds that are stable up to 800 °and under visible/UV radiation. The original aim of wet procedures based on cyanide solutions in water or methanol (MeOH) developed at the Institute of Scientific and Industrial Research (ISIR) of Osaka University was to achieve defect passivation in silicon structures for solar cells. Reaching this goal was clearly manifested [9].

In this paper we analyse optical properties of two series of silicon-based bilayers (intrinsic a-Si:H/p-type a-SiC:H and n-type mc-Si:H/intrinsic a-Si:H) deposited by PECVD on glass substrate that are common sections of p-i-n silicon solar cells. The members of both series differ by the potassium cyanide (KCN) treatment conditions. The influence of three regimes of KCN treatment on effective optical properties (refractive indices, absorption coefficients and optical band gaps) of these bilayers is compared. Each bilayer was considered as one effective thin film. Then the optical properties were regarded as effective optical properties of the whole bilayer structure retrieved from transmittance measurements. To the best of our knowledge this kind of KCN effect on effective optical properties of Si-based structures has not been studied so far.

It is known that substances containing cyanide are extremely toxic for physiological systems and therefore methods for cyanide ions detection have been under considerable research [10, 11]. Optical sensing is mainly based on detecting binding sites of C-C, C-N etc. by fluorescence, absorbance or infrared spectroscopy. Here we try to show that if even no traces on these binding sites are revealed by Raman spectroscopy, UV Vis transmittance as an external experimental manifestation of optical prop-

*Institute of Aurel Stodola, Faculty of Electrical Engineering and Information Technology, University of Žilina, ul. kpt. J. Nálepku 1390, 031 01 Liptovský Mikuláš, Slovakia, **Institute of Physics, Slovak Academy of Sciences, Dúbravská cesta 9, 845 11 Bratislava, Slovakia, ***Institute of Scientific and Industrial Research of Osaka University, and CREST, Japan Science and Technology Organization, 8-1 Mihogaoka, Ibaraki, Osaka 567-0047, Japan, ⊞ Currently with the Tokyo University of Technology, 1404-1, Katakura, Hachioji, Tokyo 192-0982, Japan, mullerova@lm.uniza.sk

DOI: 10.2478/jee-2019–0045, Print (till 2015) ISSN 1335-3632, On-line ISSN 1339-309X

erties is sensitive to the influence of cyanide treatment in case of small concentrations of KCN in solutions.

2 Experimental

The following Si based bilayers were deposited by PECVD on cleaned Corning 7059 glass:

- Bilayer A: i a-Si:H/p a-SiC:H
- Bilayer B: n mc-Si:H/i a-Si:H

These bilayers represent segments of common p-i-n thin film amorphous silicon solar cells with intrinsic hydrogenated a-Si:H as a solar absorber. In investigated bilayers intrinsic a-Si:H is accompanied by p-doped amorphous hydrogenated silicon carbide (a-SiC:H) or n-doped microcrystalline hydrogenated silicon (mc-Si:H).

The deposition was performed by commercial Samco PDM-304N PECVD apparatus at rf power density of 0.03 $W cm^{-2}$ [9]. For the intrinsic a-Si:H deposition the gas mixture of SiH_4 diluted by H_2 (at the pressure of 120 Pa) was applied. For deposition of a p-type a-SiC:H layer and and n-type mc-Si:H layer the gas mixtures of SiH_4, B_2H_6 (500 ppm, diluted by H_2), CH_4 (10% diluted by H_2) and H_2, and that of SiH_4, PH_3 (500 ppm, diluted by H_2) and H_2, respectively, were used (at a pressure of 133 Pa). The rf power densities were 0.05 and 0.04 $W cm^{-2}$ for the p-type a-SiC and n-type mc-Si depositions, respectively. The estimated thickness of intrinsic a-Si:H layer was $\sim$ 400 – 600 nm, the thickness of the n- and p-doped layers $\sim$ 30 – 50 nm.

After the deposition three different KCN treatments were applied for 2 minutes (Table 1) for the investigation of the KCN effect on optical transmittances and optical properties and for the comparison with each other and the reference samples.

Table 1. The scheme of KCN treatments of bilayers A and B

	Solution	Solution temperature
1	0.1 M KCN aqueous	RT
2	0.1 M KCN MeOH	RT
3	0.1 M KCN MeOH	Boiling

The Raman scattering spectra were recorded by THERMO SCIENTIFIC DXR Raman spectrometer in the wavenumber range of (4000 – 250) cm^{-1} under excitation by laser radiation of the wavelength of 532 nm and power of 5 mW. Optical transmittances at nearly normal incidence were measured in the spectral range of (400 – 1100) nm by UV/Vis AvaSpec-2048 spectrophotometer with air blank reference channel.

Prior information of similar samples deposited on glass and crystalline Si substrates was gathered by FTIR spectroscopy and photoluminescence [9, 12-14]. Si-CN binding revealed by FTIR was reported. Application of boiling KCN solutions considerably increases amplitudes of photoluminescence signals coming from a-Si based bilayers with maximum observed for the samples immersed in boiling MeOH KCN solution. This effect can be related to the reduction of non-radiative transitions in excited region of amorphous structures due to passivation of corresponding defect states in a-Si structures in boiling KCN solutions [9].

3 Results and discussion

3.1 Raman scattering

Raman scattering spectra can be seen in Fig. 1, 2 with the vibration mode assignments. In the spectral range over 2200 cm^{-1} no specific features were recorded. Prominent features are phononic silicon modes labelled as TO (transverse optical), LA (longitudinal acoustic) and LO (longitudinal optical). Other features in Raman scattering spectra can be classified as Si-H bond vibrations. Unfortunately no bonds with carbon or nitrogen can be identified in spectra. Therefore we conclude that Raman scattering spectroscopy was not sensitive enough to detect cyanide ions bonding in investigated Si bilayers.

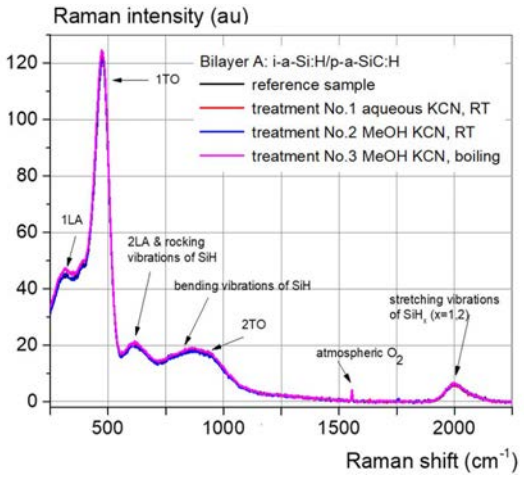

Fig. 1. Raman scattering spectra of reference and KCN treated bilayer A: intrinsic a-Si:H/p-type a-SiC:H

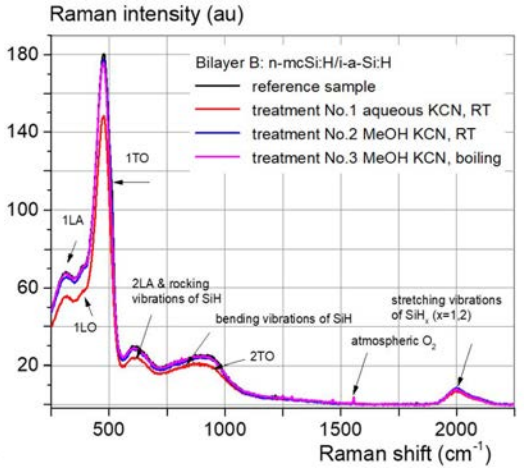

Fig. 2. Raman scattering spectra of reference and KCN treated bilayer B: n-type mc-Si:H/intrinsic a-Si:H

In spectra of the bilayer A no special difference between line shapes and positions can be seen between reference and KCN treated samples. The bilayer B shows more sensitivity of Si bonding caused by KCN MeOH treatment. In general the integrated intensities of the distinct TO peak at $\sim$480 cm^{-1} decrease after KCN treatment which can be attributed to increasing structural disorder in the samples.

3.2 Transmittance spectra

Transmittance spectra of the reference and KCN treated bilayers A, B are Fig. 3, 4. The absorption edge seems to be quite resistant to KCN treatments. Apparent interference fringes come from the partial transparency of the samples above the absorption edge.

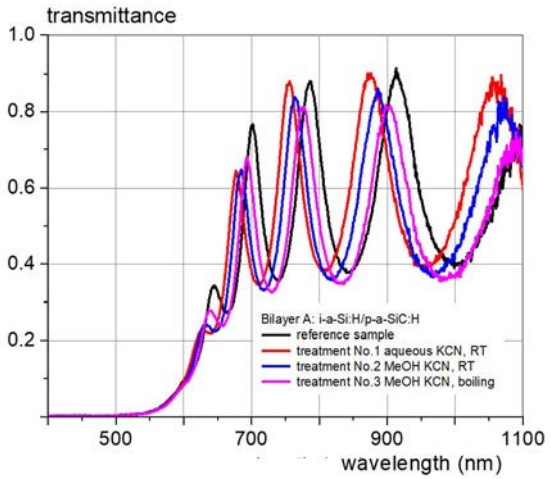

Fig. 3. Transmittance of reference and KCN treated bilayer A: intrinsic a-Si:H/p-type a-SiC:H

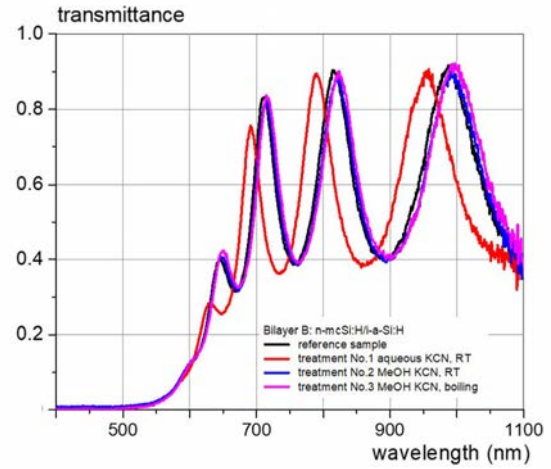

Fig. 4. Transmittance of reference and KCN treated bilayer B: n-type mc-Si:H/intrinsic a-Si:H

It is known that differences in transmittance spectra of thin films stem from different thickness and optical properties (refractive index, absorption coefficient). In general, retrieving optical parameters from experimental data requires the modelling of the light propagation in the structures which corresponds to multiple coherent transmissions and reflections.

The structures under study are built as planar bilayers. However the measured transmittance as an external optical property can be seen as a demonstration of the transmittance of one composite homogeneous thin film constituted from a bilayer representing effective medium. From transmittance spectra refractive indices and extinction coefficients of this equivalent effective thin film can be retrieved. The retrieved parameters of one effective single thin film must correspond to the light propagation, *ie* measured transmittance.

Transmittance $T(\lambda)$ as a function of the wavelength λ of a homogeneous thin film with parallel interfaces deposited on a thick substrate is a nonlinear function of the wavelength, refractive indices and extinction coefficients of the film and substrate and of the film thickness. Refractive indices n and extinction coefficients k as real and imaginary parts of the complex refractive index $\tilde{n} = n+ik$ can be extracted from the numerical comparison of $T(\lambda)$ and measured transmittance $T_{\exp}(\lambda)$. Global optimization procedure based on genetic algorithm minimizing differences between the experimental and theoretical transmittance was used in the broad spectral region including the vicinity of the absorption edge. The theoretical transmittance $T(\lambda)$ to be compared with the experiment was calculated using the theory in [15] and the Tauc-Lorentz dispersion model for $n(\lambda)$, $k(\lambda)$ widely accepted for the parameterization of the optical functions of amorphous and microcrystalline semiconductors [16]. The absorption coefficient α related to k as $\alpha = 4\pi k/\lambda$ brings usually more descriptive information about absorptive properties of a material as the original extinction coefficient k.

The refractive indices versus the wavelength and absorption coefficients versus the photon energies $E_{phot} = hc/\lambda$ (h is the Plancks constant, c is the speed of light) of the reference and KCN treated bilayers A and B considered as effective optical parameters are in Fig. 5 - 8. The effective thicknesses d of the bilayers considered as one effective film determined from the above described procedure are in Table 2.

After KCN treatment changes in refractive indices can be seen that are related to the absorption edge at the wavelengths $\sim$400 nm due to the Kramers-Kronig causality. By extrapolating spectral refractive indices to the non-absorbing region the so-called refractive index in the long wavelength limit n_∞ can be received. The values of n_∞ in Table 2 obtained by extrapolation of n (Fig. 5, 7) to the infrared region ($\lambda \sim$ 2000 nm) display the changes brought about by KCN treatments. MeOH KCN treatments (No.2 and 3) cause the increase of n_∞ of the bilayer A indicating that the material becomes more compact. The densification means that vacancies in amorphous films are filled and the effective thickness d is decreased (Table 2). Effective thickness shrinkage (except for boiling MeOH KCN treatment) was observed. The increase of the refractive index of the bilayer B after KCN treatment is observed only after treatments at room temperature. The effective thickness shrinkage is recognized

Table 2. Effective thicknesses d of the whole structures considered as one effective thin film determined from fitting transmittance spectra. Refractive index in the long-wavelength limit n_∞, optical path length Λ and the change of the optical path length $\Delta\Lambda$ versus the reference sample.

No.	Bilayer A d (nm)	Bilayer A n_∞ (–)	Bilayer A Λ (nm)	Bilayer A $\Delta\Lambda$ (nm)	Bilayer B d (nm)	Bilayer B n_∞ (–)	Bilayer B Λ (nm)	Bilayer B $\Delta\Lambda$ (nm)
Ref.	630	3.53	2224	–	570	3.39	1932	–
1	600	3.48	2088	−136	535	3.48	1861	−71
2	580	3.68	2134	−90	565	3.43	1938	+6
3	575	3.80	2185	−39	580	3.36	1949	+17

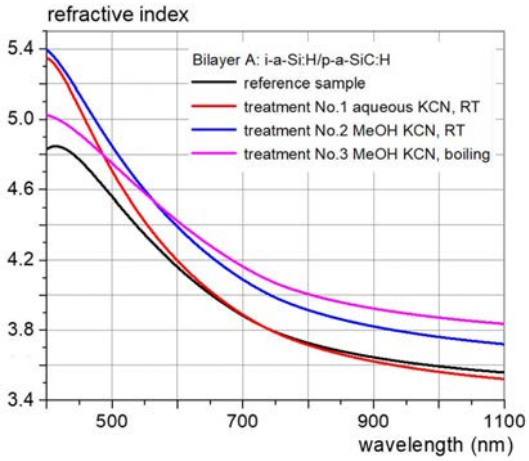

Fig. 5. Effective refractive indices of the bilayer A

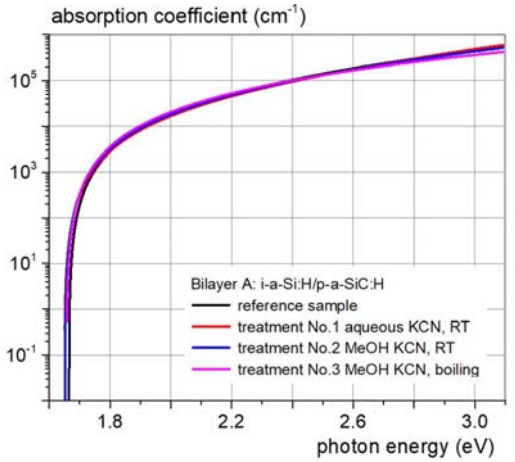

Fig. 6. Effective absorption coefficients of the bilayer A

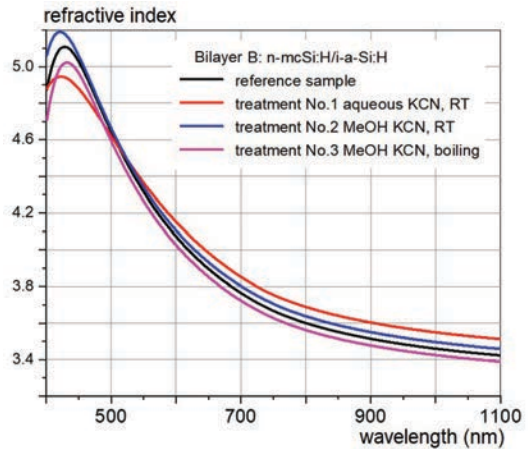

Fig. 7. Effective refractive indices of the bilayer B

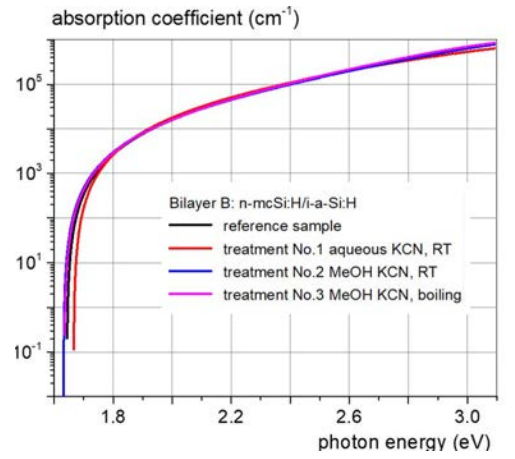

Fig. 8. Effective absorption coefficients of the bilayer B

only after treatment by aqueous KCN solution at room temperature. In general lower refractive indices of the bilayer B represents less dense material with the distribution crystalline grains, grain boundaries and voids sensitive to KCN treatments.

Knowing the thickness d of the effective thin film and the refractive index in the long-wavelength limit n_∞, we can calculate the optical path length $\Lambda = n_\infty d$ that an unabsorbed perpendicularly incident solar radiation will travel in the bilayer. Λ and the differences $\Delta\Lambda$ against the reference sample corresponding to KCN treated samples are in Table 2. It is obvious that KCN treatment of the bilayer A causes the reduction of the optical path length, while MeOH KCN treatment of the bilayer B

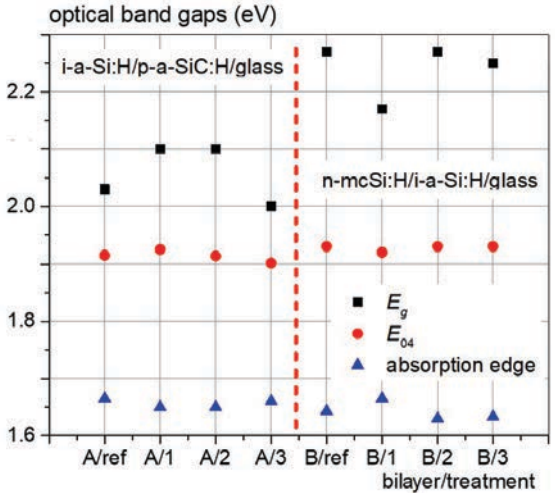

Fig. 9. Comparison of the effect of KCN treatment on optical band gaps

brings slight optical path length enhancement. The results in Table 2 correspond well to the published data on the changes of the effective optical path length calculated by different methodology from FTIR spectra [12].

In thin film solar cells the optical path length enhancement connected with the so-called light trapping is highly required and various effective concepts have been applied so far [17]. The only but deficient enhancements of Λ were achieved for the KCN MeOH treated bilayer B ($+\Delta\Lambda$ in Table 2). In all resting cases an undesirable reduction of Λ occurs. However, we conclude that this issue must also be taken into account to consider the overall effects of KCN treatments in solar cell materials.

The absorption coefficients do not reveal specific changes due to KCN treatments except for the vicinity of the absorption edge, i.e. at photon energies < 1.8 eV where absorption coefficients are partly influenced.

The absorption edge is defined as the sharp abrupt in the absorption spectrum, i.e. a discontinuity in the plot of the absorption coefficient versus the photon energy. The intersection of the extrapolated absorption coefficient with the abscissa can be resolved from Fig. 6, 8. However due to disorder in amorphous/microcrystalline semiconductors the valence and conduction band edges are extended with rather vague abrupt energy above which photons are absorbed via interband transitions. Then the so-called Tauc plot is a conventional method for calculating the band gap energies. Related optical band gaps can be determined from the extrapolation of linear parts of Tauc plots $\alpha E_{phot} \sim (E_{phot} - E_g)^2$ (E_g is the Tauc optical band gap) to the energy axis. Absorption edges and optical band gaps of effective thin films representing investigated bilayers are depicted in Fig. 9. To avoid the ambiguity in determining optical band gaps in case of reduced linear parts of Tauc plots the so-called iso-absorption gap E_{04} is occasionally used defined as the photon energy at which the absorption coefficient achieves the value of $10^4\,\mathrm{cm}^{-1}$. Here it is clear from Fig. 6 and 8 that E_{04} is not reflecting particular differences in optical absorption and remains almost the same after KCN treatments. This conclusion can be seen clearly in Fig. 9.

4 Conclusions

Optical properties of two silicon based bilayers (intrinsic a-Si:H/p-type a-SiC:H and n-type mc-Si:H/intrinsic a-Si:H) were investigated before and after treatment in aqueous and MeOH KCN solutions. Dispersive and absorptive optical properties – refractive indices, absorption coefficients and optical band gaps were determined from transmittance spectra under consideration of each bilayer as one effective thin film with effective optical properties. After KCN treatments optical properties were modified probably due to the structural changes of bilayers. Refractive indices of intrinsic a-Si:H/p-type a-SiC:H apparently increase after MeOH KCN treatment. The bilayer of n-type mc-Si:H/intrinsic a-Si:H acquires increased refractive indices after KNC treatment at room temperature no matter what solvent was used. Definitely UV Vis transmittance and retrieved optical properties showed sensitivity to the influence of cyanide treatment in case of small concentrations of KCN in solutions. For this reason the possibility of sensing KCN using affected optical properties could be appealing.

Acknowledgements

This work was partly supported by the Slovak Research and Development Agency under the projects APVV-15-0152 and APVV-17-0631. The results were partially developed by Slovak Grant Agency under the projects VEGA 1/0840/18, VEGA 2/0149/18 and by European Union's Horizon 2020 Research and Innovation Programme under the Marie-Skodowska-Curie Grant Agreement No. 734331.

References

[1] S. Wagner, "Thin-film semiconductors – From exploration to application", *MRS Bulletin*, vol. 43, pp. 617–624, 2018.

[2] P. Calta, P. Šutta, R. Medlín, M. Netrvalová, "Impact of sublayer thickness and annealing on silicon nanostructures formation in a-Si:H/a-SiNx:H superlattices for photovoltaics", *Vacuum*, vol. 153, pp. 154–161, 2018.

[3] H. Aguas, S. K. Ram, A. Araujo, D. Gaspar, A. Vicente, S. A. Filonovich, E. Fortunato, R. Martins, I. Ferreira, "Silicon thin film solar cells on commercial tiles", *Energy Environ. Sci.*, vol. 4, pp. 4620–4632, 2011.

[4] C. Wronski, "The limited relevance of SWE dangling bonds to degradation in high-quality a-Si:H solar cells", *IEEE J. Photovolt.*, vol. 4, pp. 778–784, 2014.

[5] N. E. Grant, J. D. Murphy, "Temporary surface passivation for characterisation of bulk defects in silicon: A Review", *Phys. Stat. Sol. RRL*, vol. 11, pp. 1700243, 2017.

[6] M. Takahashi, T. Shishido, H. Iwasa, H. Kobayashi, "Passivation of defect states in surface and edge regions on pn-junction Si solar cells by use of hydrogen cyanide solutions", *Central Eur. J. Phys.*, vol. 7, pp. 227–231, 2009.

[7] M.-H. Kim, M.-J. Choi, K. Kimura, H. Kobayashi, D.-K. Choi, "Improvement of the positive bias stability of a-IGZO TFTs by

the HCN treatment", *Solid-State Electron.*, vol. 126, pp. 87–91, 2016.

[8] Ch.-Ch. Chao, Y.-H. Hu, Ch.-Ch. Lai, J.-Y. Chang, "Defects reduction of amorphous silicon thin film in cyanide solution treatment", *IEEE Proc. Of* 4^{th} *IEEE Int. NanoElectronics Conf.*, 2011.

[9] E. Pinčík, H. Kobayashi, J. Rusnák, M. Takahashi, M. Mikula, W. B. Kim, M. Kučera, R. Brunner, S. Jurečka, "Passivation of Si-based structures in HCN and KCN solutions", *Appl. Surf. Sci.*, vol. 258, pp. 8397–8405, 2012.

[10] M. La, Y. Hao, Z. Wang, G.-Ch. Han, L. Qu, "Selective and Sensitive Detection of Cyanide Based on the Displacement Strategy Using a Water-Soluble Fluorescent Probe", *J. Analyt. Methods in Chemistry*, vol. 2016, pp. 1462013, 2016.

[11] B. Barare, I. Babahan, Y. M. Hijji, E. Bonyi, S. Tadesse, K. Aslan, "A Highly Selective Sensor for Cyanide in Organic Media and on Solid Surfaces", *Sensors*, vol. 16, pp. 271, 2016.

[12] E. Pinčík, R. Brunner, H. Kobayashi, M. Takahashi, M. Mikula, "Interaction of KCN solutions with Si-based thin films", *J. Chin. Adv. Mater. Soc.*, vol. 3, pp. 119–127, 2015.

[13] M. Kopáni, M. Mikula, N. Fujiwara, M. Takahashi, E. Pinčík, "The effect of KCN passivation on IR spectra of a-Si based structures", *Appl. Surf. Sci.*, vol. 258, pp. 8406–8408, 2012.

[14] R. Brunner, E. Pinčík, M. Kučera, M. Mikula, "Photoluminescence investigation of thin film a-Si:H based structures passivated in cyanide solution", *J. Chin. Adv. Mater. Soc.*, vol. 4, pp. 62–69, 2015.

[15] J. Müllerová, P. Šutta, "On some ambiguities of the absorption edge and optical band gaps of amorphous and polycrystalline semiconductors", *Communications*, vol. 3, pp. 9–15, 2017.

[16] G. E. Jellison, Jr., F. A. Modine, "Parametrization of the optical functions of amorphous materials in the interband region", *Appl. Phys. Lett.*, vol. 69, pp. 371–373, 1996.

[17] A. N. Sprafke, R. B. Wehrspohn, "Current Concepts for Optical Path Enhancement in Solar Cells", *Photon Management in Solar Cells, First Edition*, Wiley-VCH Verlag GmbH & Co. KGaA, 2015.

Received 19 March 2019